Mass transfer effects in plating reactors

G. Nelissen, B. Van Den Bossche, A. Van Theemsche, J. Deconinck
Vrije Universiteit Brussel, Department of Electrical Engineering TW/ETEC

Mass transfer effects can drastically influence the behavior of plating reactors. In this paper a simulation tool is presented to analyze the fluid flow in arbitrary shaped electrochemical reactors. Using this flow field, the local mass transfer at high Schmidt numbers, including effects of electrode reactions, will be calculated. Some examples are shown to illustrate the effects of the laminar and turbulent fluid flow, the geometry and the Schmidt number on the performance of the plating cell. The results of the calculations are compared with measured values of the local mass transfer coefficients.

For more information, contact:
Gert Nelissen
Vrije Universiteit Brussel
Department of Electrical Engineering TW/ETEC
Pleinlaan, 2
B-1050 Brussels
BELGIUM

Phone: +32 (0)2 6292811
Fax: +32 (0)2 6293620
E-mail: gnelisse@vub.ac.be

Introduction

One of the most important factors in the behaviour of plating reactors is the local mass transfer. This local mass transfer is mainly determined by the electrolyte flow in the reactor. To optimise a plating reactor, an accurate prediction of the local mass transfer and thus the fluid flow is needed.

In this paper, a numerical model is presented to calculate the laminar and turbulent fluid flow and mass transfer in arbitrary shaped reactors. Some simulations of a parallel plate reactor are shown, together with a validation of the results by comparison with correlations found in literature. Furthermore, a calculation including the effects of electrode reactions is presented, which allows assessing the behaviour of the reactor for different fractions of the limiting current.

Fluid flow model

Navier-Stokes equations

The equations describing the (laminar) incompressible fluid flow are the Navier-Stokes equations, describing the conservation of mass:

$$\frac{\partial U_i}{\partial x_i} = 0 \tag{1}$$

and the conservation of momentum :

$$\rho \frac{\partial U_i}{\partial t} + \rho U_j \frac{\partial U_i}{\partial x_j} = -\frac{\partial p}{\partial x_i} + \frac{\partial(\tau_{ji})}{\partial x_j} \tag{2}$$

with x_i the space coordinates , U_i the velocity components, p the pressure, t the time, ρ the density, τ_{ij} the viscous stresses given by :

$$\tau_{ij} = 2\mu S_{ij} \tag{3}$$

with, for Newtonian fluids, μ the molecular viscosity and S_{ij} the strain-rate given by :

$$S_{ij} = \frac{1}{2}\left(\frac{\partial U_i}{\partial x_j} + \frac{\partial U_j}{\partial x_i} \right). \tag{4}$$

Solution of these equations together with the appropriate boundary conditions will yield the flow field in an arbitrary shaped geometry.

Reynolds Averaged Navier-Stokes Equations

One possible way of equations turbulent fluid flow is based on the Reynolds Averaged Navier-Stokes equations :

$$\frac{\partial U_i}{\partial x_i} = 0 \tag{5}$$

$$\rho \frac{\partial U_i}{\partial t} + \rho U_j \frac{\partial U_i}{\partial x_j} = -\frac{\partial p}{\partial x_i} + \frac{\partial(\tau_{ij} + \tau_{ji})}{\partial x_j}. \tag{6}$$

The turbulent stresses (Reynolds stresses) τ_{ij} are given by

$$\tau_{ij} = 2\mu_t S_{ij} - \frac{2}{3}\rho k \delta_{ij}, \tag{7}$$

with μ_t. the turbulent viscosity, which in contrast to the molecular viscosity is not a property of the fluid but of the flow. The variable k is the specific turbulent kinetic energy equal to half the fluctuating velocity components u_i' :

$$k = \frac{1}{2} u_i' u_i' \tag{8}$$

The factor $\frac{2}{3}$ in equation (7) only holds for the 3 dimensional case. In 2 dimensions this factor becomes 1.

A derivation and a much more detailed description of these equations can be found in the book of Wilcox[1]. Also a very extended overview of the different turbulence models, together with their advantages and disadvantages can be found in the same reference.

The net result of the above is that one can define an 'apparent' viscosity defined as the sum of the molecular viscosity μ and the turbulent viscosity μ_t :

$$\mu_{apparent} = \mu + \mu_t \tag{9}$$

and use this apparent viscosity in the Navier-Stokes equations.

Turbulence models

The aim of all turbulence models is to describe the local variation of the turbulent (eddy) viscosity μ_t. Mainly, there are 3 commonly used types of turbulence models :

- Algebraic models. Based on the mixing length hypothesis, these models express an algebraic relation between the turbulent viscosity and some length scales of the mean flow. They are by definition incomplete, because they always need additional case-specific input. The most commonly used algebraic models are the Cebeci-Smith and the Baldwin- Lomax model.
- One-equation models. These models postulate that the turbulent viscosity depends upon the kinetic energy of the turbulent fluctuations k. The most commonly used one-equation model is the Spalart-Almaras model.
- Two-equation models. k-ε, k-ω and their variants are the most commonly used two-equation turbulence models. They are complete as the can predict properties of a given turbulent flow with no prior knowledge of the turbulence structure.

In this work the k-ω model was chosen because of its good performance in predicting mass transfer, as no wall functions are needed. This allows an integration of the complete set of equations through the viscous sub-layer without any further approximations.

k-ω turbulence model

The k-ω model has been developed by Kolmogorov in 1942. It describes the turbulent kinetic energy k and the dissipation of the turbulent kinetic energy per volume and per time unit ω. In this work only the 'Low Reynolds' version of the k-ω model has been used, as we are only interested in industrial flows in plating reactors (up to Re = 500000).

Wilcox gives the following version of the 'Low Reynolds' k-ω model :
Turbulent kinetic energy (k)

$$\frac{\partial k}{\partial t} + U_j \frac{\partial k}{\partial x_j} = \tau_{ij} \frac{\partial U_i}{\partial x_j} - \beta^* k\omega + \frac{\partial}{\partial x_j}\left[(\mu + \sigma^* \mu_t) \frac{\partial k}{\partial x_j} \right] \tag{10}$$

Dissipation (ω)

$$\frac{\partial \omega}{\partial t} + U_j \frac{\partial \omega}{\partial x_j} = \alpha \frac{\omega}{k} \tau_{ij} \frac{\partial U_i}{\partial x_j} - \beta \omega^2 + \frac{\partial}{\partial x_j}\left[(\nu + \sigma \nu_t) \frac{\partial \omega}{\partial x_j} \right] \tag{11}$$

Turbulent viscosity

$$\nu_t = \alpha^* \frac{\rho k}{\omega} \tag{12}$$

Turbulent Reynolds number

$$\mathrm{Re}_T = \frac{k}{\nu \omega} \tag{13}$$

Coefficients and damping functions

$$\alpha^* = \frac{\alpha_0^* + \mathrm{Re}_T / R_k}{1 + \mathrm{Re}_T / R_k} \tag{14}$$

$$\alpha = \frac{13}{25} \frac{\alpha_0 + \mathrm{Re}_T / R_\omega}{1 + \mathrm{Re}_T / R_\omega} (\alpha^*)^{-1} \tag{15}$$

$$\beta^* = \frac{9}{100} \frac{4/15 + \left(\mathrm{Re}_T / R_\beta\right)^4}{1 + \left(\mathrm{Re}_T / R_\beta\right)^4} f_{\beta^*} \tag{16}$$

$$\beta = \frac{9}{125} f_\beta, \ \sigma^* = \sigma = \frac{1}{2}, \ \alpha_0^* = \frac{1}{3} \beta_0, \ \alpha_0 = \frac{1}{9} \tag{17}$$

$$R_\beta = 8, \ R_k = 6, \ R_\omega = 2.95 \tag{18}$$

$$f_\beta = 1, \ \chi_k = \frac{1}{\omega^3} \frac{\partial k}{\partial x_j} \frac{\partial \omega}{\partial x_j} \tag{19}$$

$$f_{\beta^*} = \begin{cases} 1 & \chi_k \le 0 \\ \dfrac{1 + 680 \chi_k^2}{1 + 400 \chi_k^2} & \chi_k > 0 \end{cases} \tag{20}$$

Together with the appropriate boundary conditions, these equations allow to calculate the turbulent flow in an arbitrary shaped geometry. However, no model will yield the 'exact' fluid flow in all cases.

Turbulent mass transfer

The limiting current density distribution in a laminar flow is given the laminar convection-diffusion equation:

$$U_j \frac{\partial C}{\partial x_j} = \frac{\partial}{\partial x_j}\left[D_{mol} \frac{\partial C}{\partial x_j} \right] \tag{21}$$

with U_j the velocity components calculated as described above, C the concentration and D_{mol} the molecular diffusion constant. Similar as for the fluid flow, one can extend this equation for turbulent flow as:

$$U_j \frac{\partial C}{\partial x_j} = \frac{\partial}{\partial x_j}\left[(D_{mol} + D_T) \frac{\partial C}{\partial x_j} \right] \tag{22}$$

with D_T the turbulent diffusion.

For mass transfer the following dimensionless numbers are commonly used:

$$Sc = \frac{\boldsymbol{n}}{D_{mol}} \tag{23}$$

the Schmidt number, equivalent to the Prandtl number in heat transfer, describing the ratio between the viscosity and the molecular diffusion;

$$Sc_T = \frac{\boldsymbol{n}_T}{D_T} \tag{24}$$

the turbulent Schmidt number, equivalent to the turbulent Prandtl number, describing the ratio between the turbulent viscosity and the turbulent diffusion.

Turbulence models for mass transfer

In literature[2,3,6,7], 3 types of models are proposed for calculating the turbulent mass transfer at high Schmidt numbers :

1. $Sc_T = \infty$ (or $D_T = 0$) . It is supposed that the turbulent diffusion may be neglected because the mass transfer boundary layer for high Schmidt numbers is so small that all relevant phenomena are confined to the laminar sub-layer of the turbulent boundary layer. However, there are some strong theoretical arguments that this model is too simple and doesn't give good predictions.
2. $Sc_T = 1$. This is the straightforward extrapolation of what is generally done in turbulent heat transfer. Some authors argue that this approach is only valid for Sc number close to 1, and is invalid for high Sc numbers as encountered in electrochemical systems.
3. $Sc_T = f(\mathrm{Re}, Sc, \boldsymbol{n}, \ldots)$. The main drawback of this approach is that no single function f exists (or has been identified) that accurately predicts the turbulent mass transfer for different cases. Furthermore, f depends on some global quantities of the flow (Re, boundary layer thickness, …) which makes it difficult to extrapolate the function for non-standard cases.

In the 'Results' section, the behaviour of the models will be compared with correlations to assert the validity and applicability of the three different approaches.

Dilute solution model

The dilute solution model describes the mass and charge transfer in electrochemical reactors due to convection, diffusion, migration and homogeneous (chemical) reactions. On the electrodes, multiple electrode reactions can take place. Bortels[8] has given a detailed mathematical description.

The influence of the turbulence on the mass and charge transfer can be easily extended from the limiting current case. One turbulent Schmidt number is defined that is used to calculate the turbulent diffusion for all the species in the electrolyte.

Results

Turbulent flow in a parallel plate reactor

As a first test case the turbulent flow in a parallel plate reactor (channel) is calculated and validated with results found in literature[4,5]. The reference results are obtained from direct numerical simulation (DNS) calculations.

Figure 1 shows the geometry under investigation. The half-height of the channel is d, equal to 0.005 m. The Reynolds number, defined as :

$$\mathrm{Re} = \frac{v_{av} d}{\nu} \tag{25}$$

is equal to 3300, with v_{av} the average velocity and ν the kinematic viscosity (1E-6 m^2/s for water).

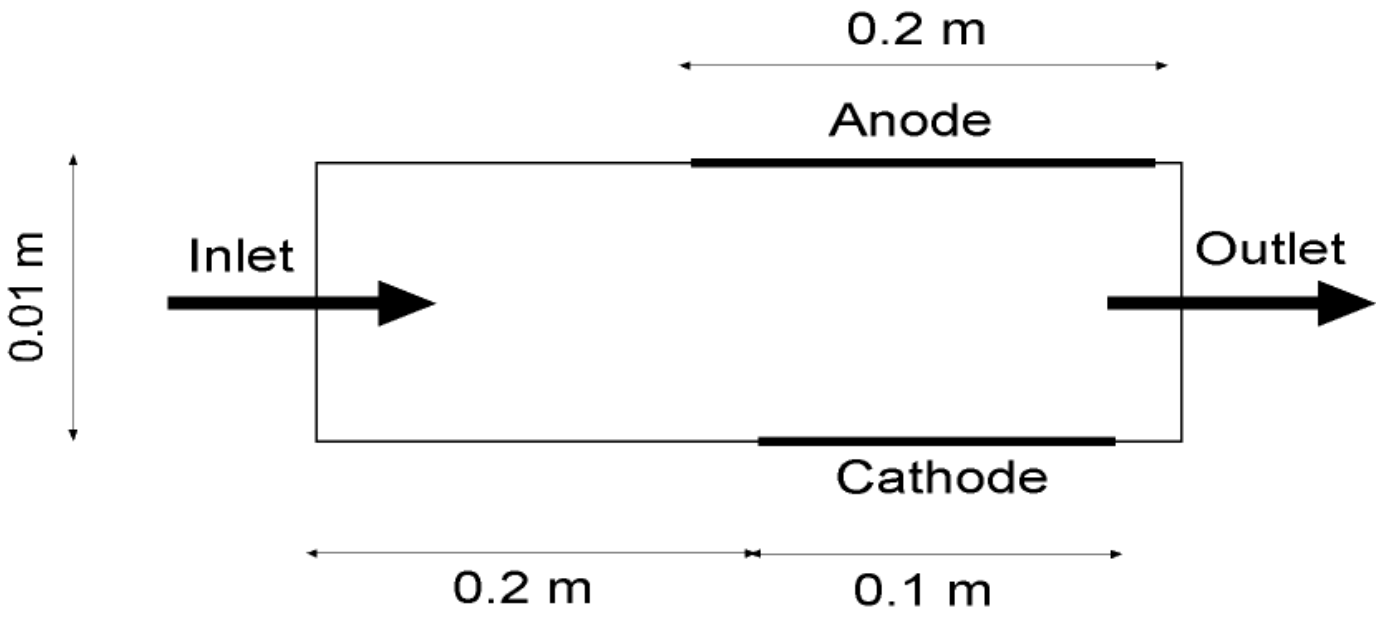

Figure 1 : Schematic drawing of the geometry of the parallel plate reactor.

The Reynolds averaged Navier-Stokes equations (5) and (6), together with the k-ω equations (10)-(20) are solved using the Finite Element method. The computational mesh, shown in Figure 2, contains 29770 triangles and 14886 points. The first element is at a distance of $y^+ = 0.05$ from the wall. Figure 3 shows a detail of the mesh near the wall. Remark the very high aspect ratio of the triangles near the wall, which allows accurate calculations, without increasing the number of triangles too much.

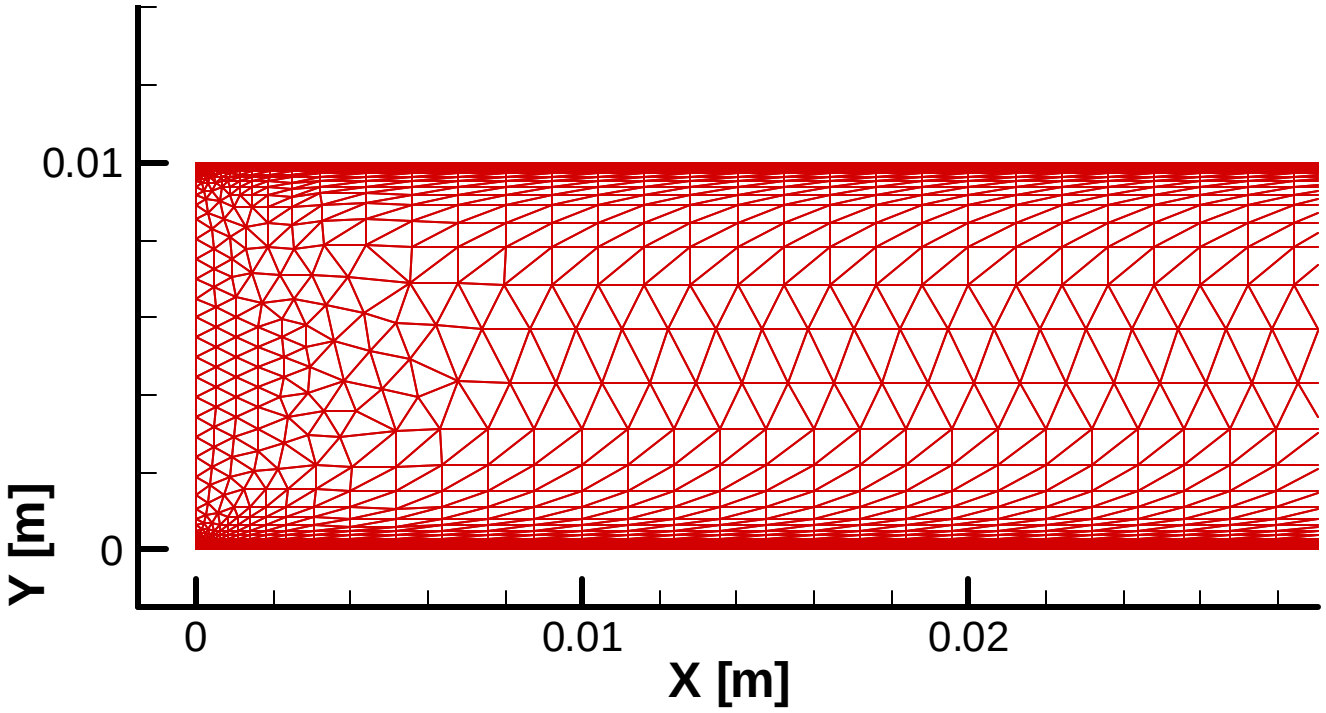

Fig. 2 - Computational mesh to solve the flow equations. It contains 29770 triangles and 14886 points.

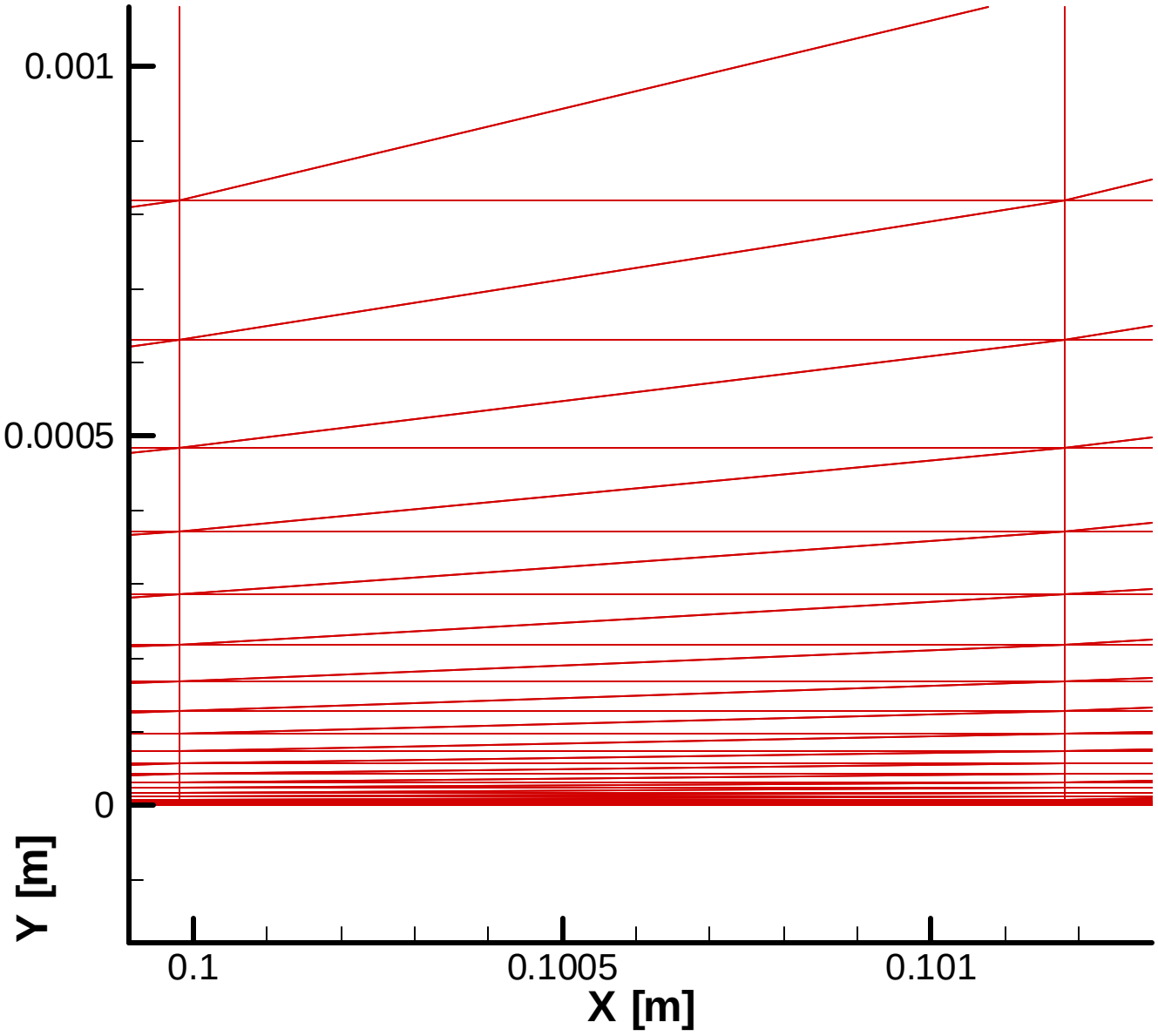

Fig. 3 – A detail of the mesh close to the wall, showing the high aspect ratio of the triangles.

Figure 4 shows the developed turbulent velocity profile in the channel. Remark that this velocity profile is much flatter then the parabolic profile found for laminar fluid flow. Furthermore, the boundary layer of a turbulent fluid flow is much smaller then of a laminar flow.

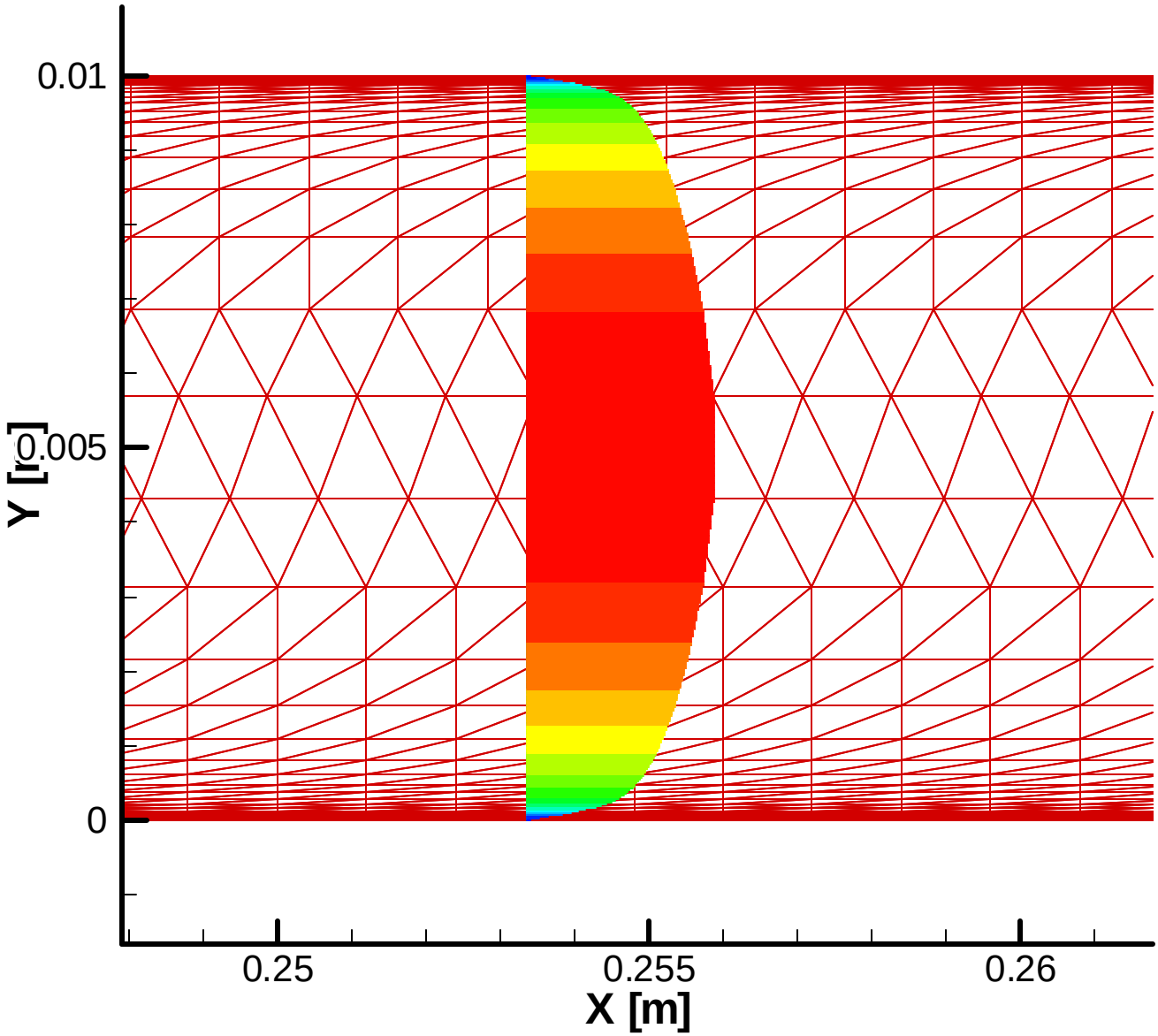

Fig. 4 – Developed turbulent velocity profile in the channel, Re = 3300.

The velocity scale (friction velocity) is defined by

$$u_t = \sqrt{\frac{\tau_{wall}}{\rho}} \qquad (26),$$

with τ_{wall} the surface shear stress as defined by (7). The dimensionless velocity and distance normal to the wall are defined as :

$$U^+ = \frac{U}{u_t} \text{ and } y^+ = \frac{u_t\, y}{\nu} \qquad (27)$$

Figure 5 compares the developed velocity profile with the reference solution. A very good agreement is observed, both for the viscous sub-layer ($y^+ < 10$) as for the log layer ($10 < y^+$). In Figure 6 the turbulent

kinetic energy profile (scaled by u_t^2) is shown. Quite a good agreement with the reference solution is obtained, especially close to the wall.

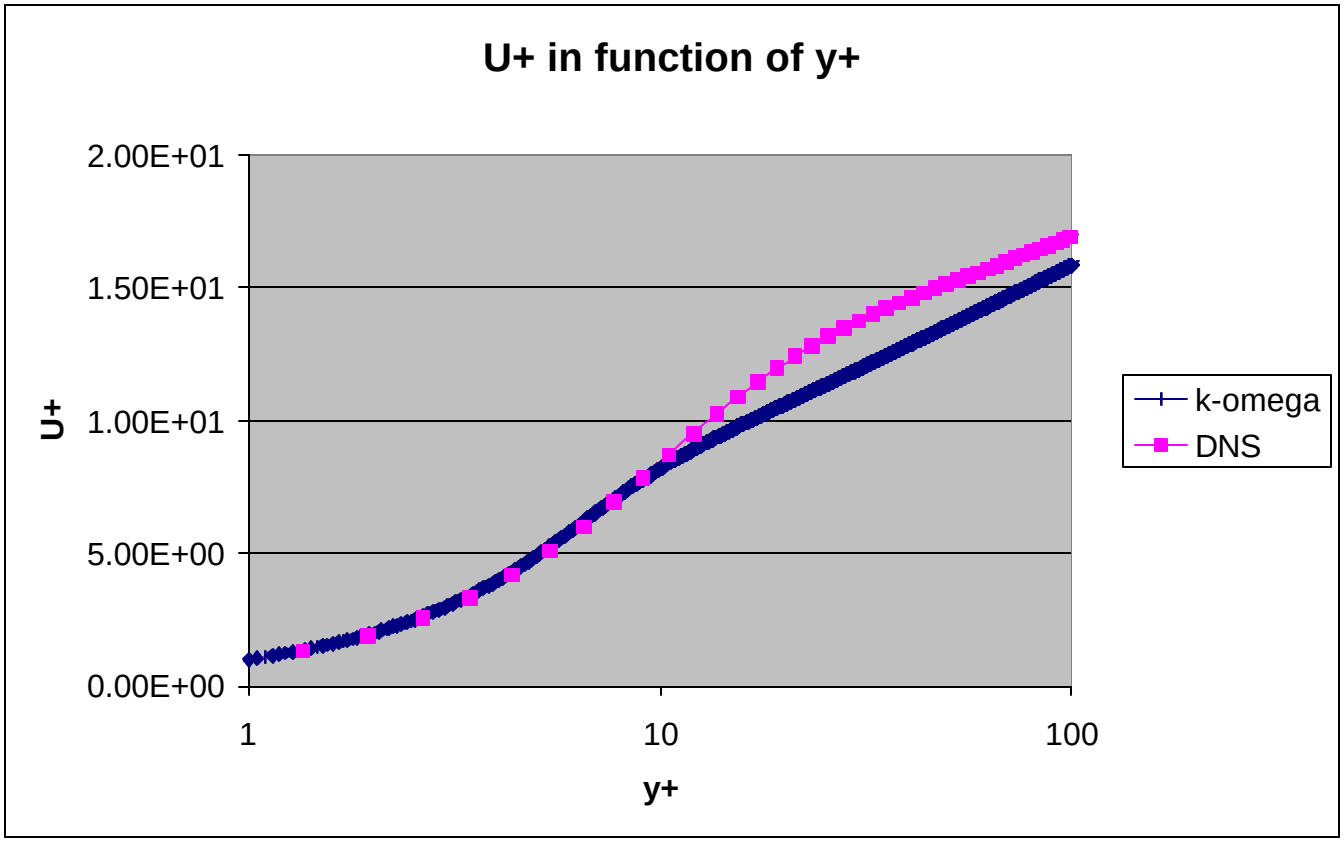

Fig. 5 – Developed turbulent dimensionless velocity profile in the boundary layer.

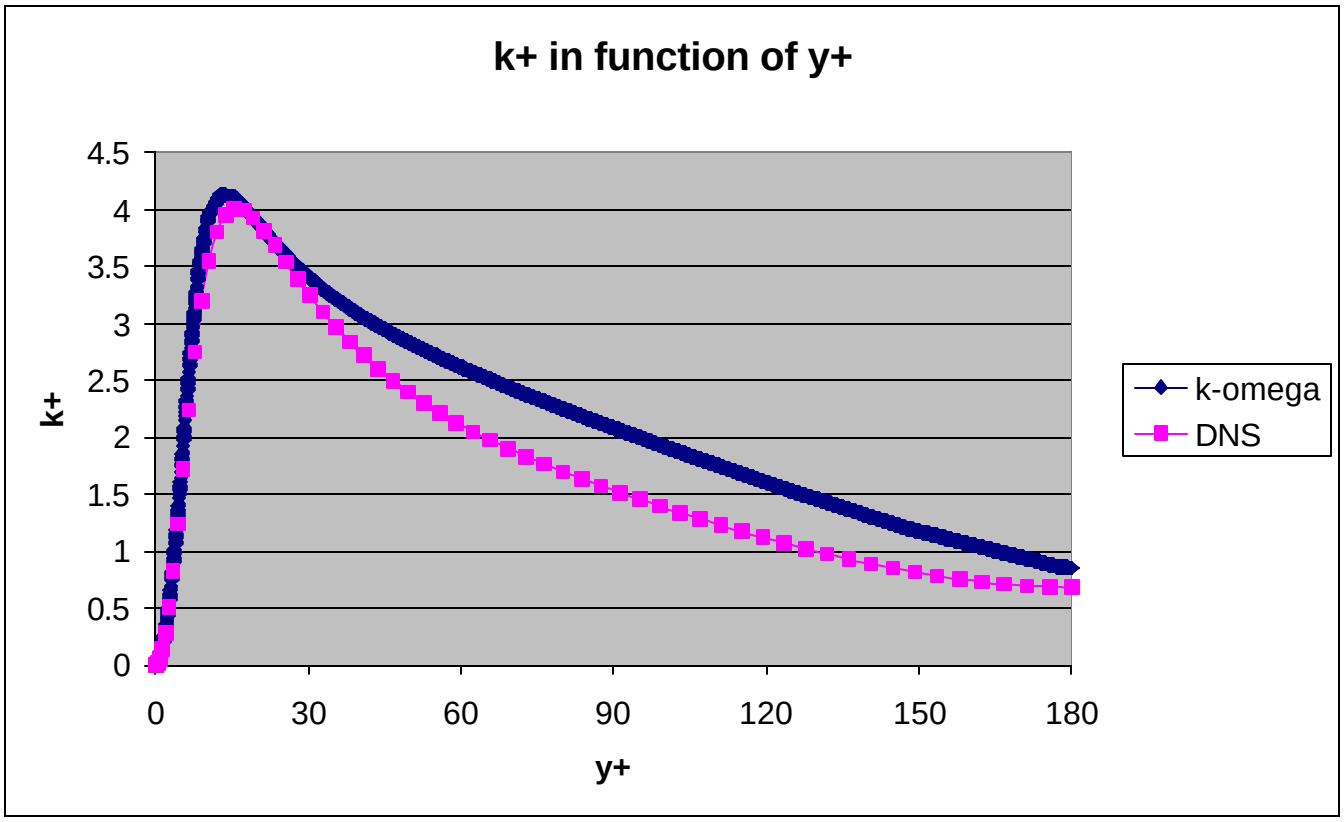

Fig. 6 – Dimensionless turbulent kinetic energy distribution normal to the wall.

Turbulent mass transfer in a parallel plate reactor at high Schmidt number

To investigate the turbulent mass transfer in a parallel plate reactor, the limiting current is calculated for different flow rates and compared with correlations found in literature. The Schmidt number is equal to 1714. The Sherwood number is related to the limiting current by:

$$Sh = \frac{I_{\lim}.d}{SnFC_b D_{mol}} \qquad (28),$$

with I_{lim} the limiting current [A], n the charge of the ion equal to 2, F the Faraday constant equal to 96487 C/mole, C_b the bulk concentration of the ion equal to 10 mole/m^3, S the surface of the cathode equal to 0.1 m^2 and D_{mol} the molecular diffusivity of the ion equal to 7.0E-10 m^2/s.

For the mass transfer in a laminar channel flow one finds the following correlation[9] for the Sherwood number :

$$Sh = 2.33\left(\frac{\mathrm{Re}\,.Sc.d}{L}\right)^{1/3} \qquad (29).$$

For the mass transfer in a turbulent channel flow, several expressions are found in literature. The most commonly used is the Chilton-Colburn[9] analogy:

$$Sh = 0.023\,\mathrm{Re}^{0.8}\,Sc^{1/3} \qquad (30).$$

Landolt[10] found the following correlation :

$$Sh = 0.022\,\mathrm{Re}^{7/8}\,Sc^{1/4} \qquad (31).$$

In the numerical simulations, three different mass transfer models are used as explained before :

- $D_T = 0$ ($Sc_T = \infty$),
- $Sc_T = 1$,
- $Sc_T = \dfrac{0.0014\left(1 - e^{(-\mathrm{Re}_{\mathrm{mod}}^{1/2}/2)}\right)}{0.001242 Sc^{-0.112}}$, with $\mathrm{Re}_{\mathrm{mod}} = 0.001(\mathrm{Re} - 3000)$ and based on the work of Rosen[6].

The results of the numerical calculations and the different correlations are shown in Figures 7 and 8. It is clear that a very good agreement between correlations and simulations is obtained for the mass transfer in laminar flow regime. Remark from these figures that, as expected, the transition from laminar to turbulent occurs at around Re = 2000.

For the turbulent mass transfer, the agreement between correlations and simulations is not very good. It is clear that the assumption $D_T = 0$ ($Sc_T = \infty$) underestimates the turbulent mass transfer and that $Sc_T = 1$ overestimates the effects of turbulence. The model of Rosen is much better in predicting the turbulent mass transfer in a channel, especially at higher Re numbers. From this it is evident, that there should exist a reasonable finite value of Sc_T for which, in this test case, the simulation matches the correlation perfectly. With some trial and error, this value was found to be $Sc_T = 4.5$. In future other tests will be done with different Sc and Re numbers and in other geometries to verify the validity of the $Sc_T = 4.5$ model.

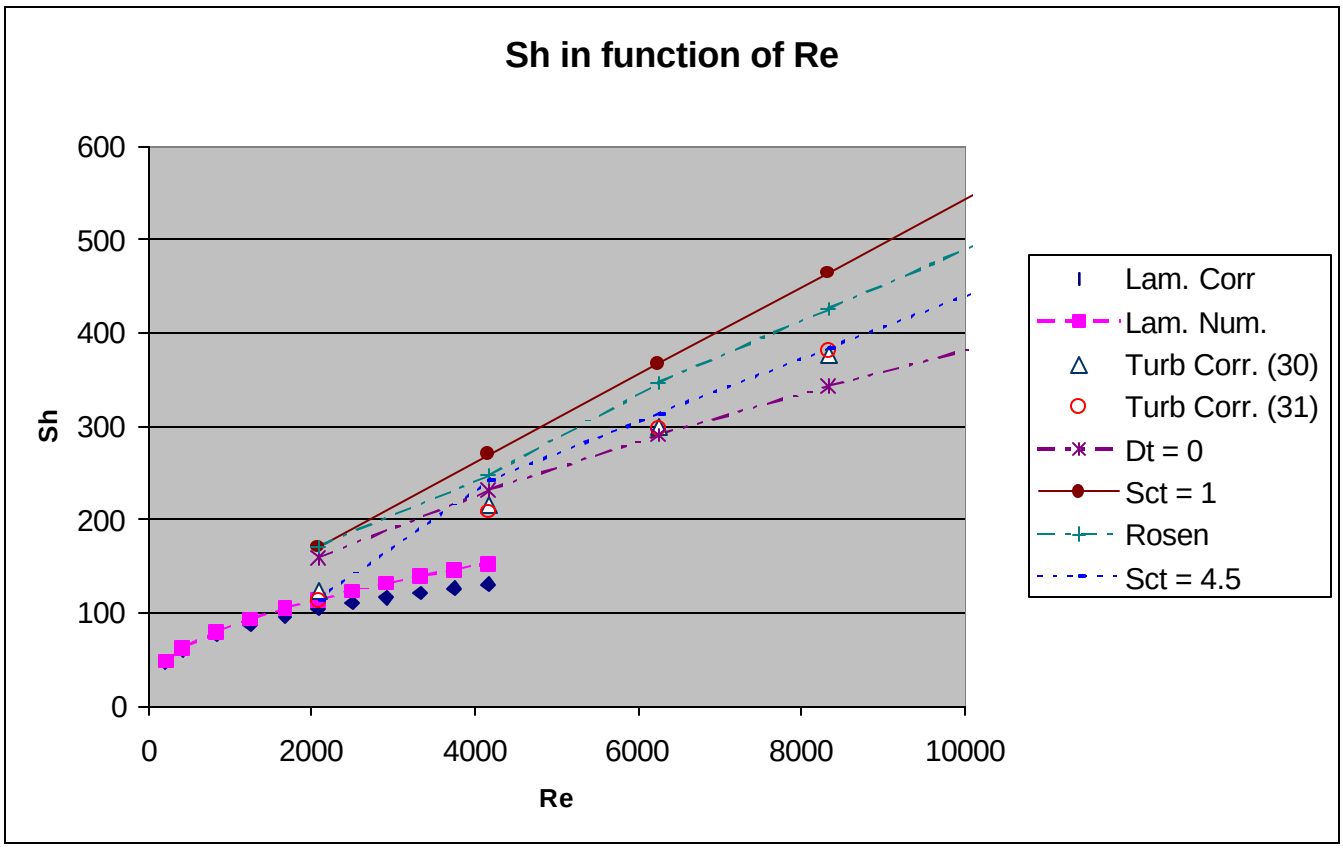

Figure 7 : Comparison of dimensionless laminar and turbulent mass transfer rate in function of the Re number from calculations with correlations.

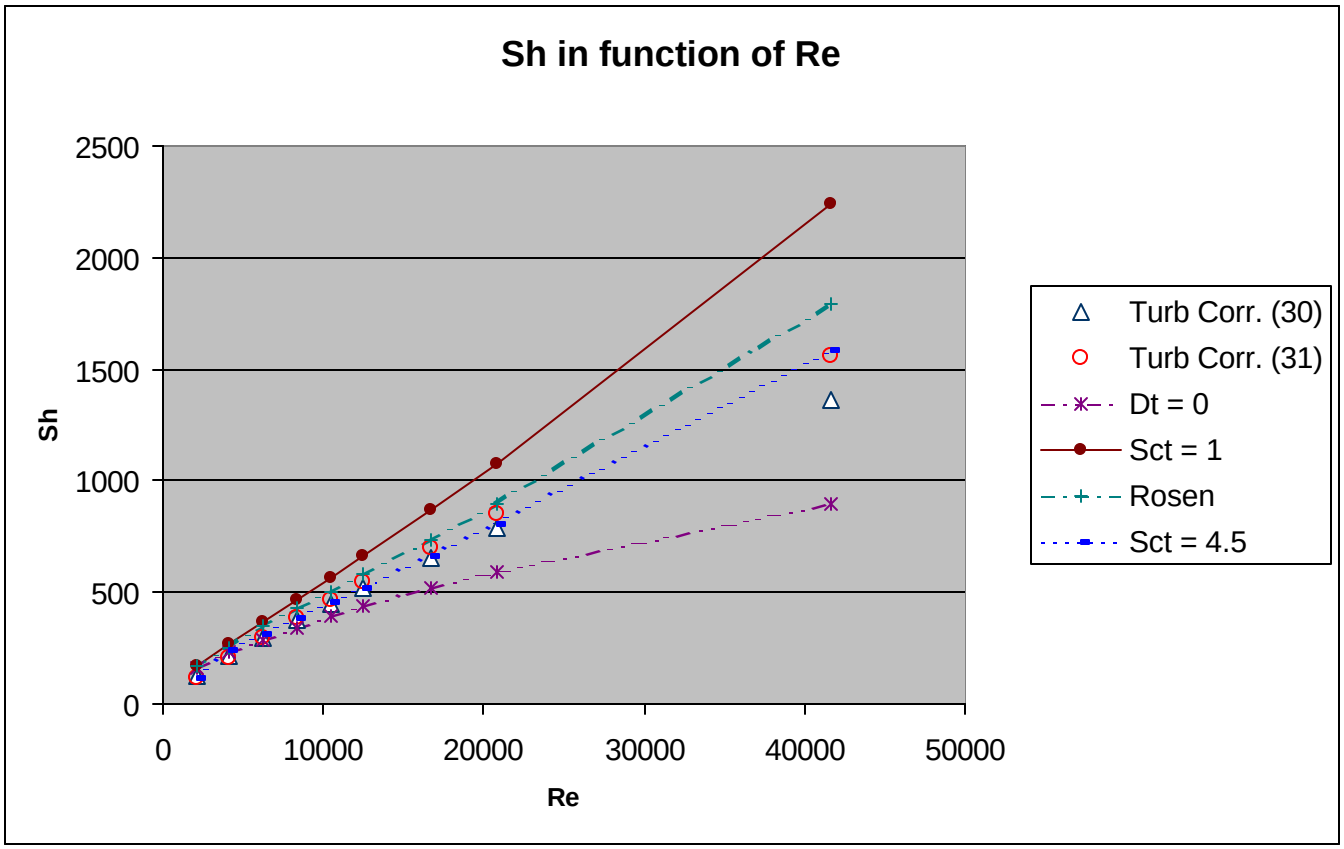

Figure 8 : Comparison of dimensionless turbulent mass transfer from calculations with correlations for Re varying from 2000 up to 42000.

Turbulent mass transfer including electrode reactions

As electrolyte a simple cupper system with properties shown in Table 1 is used.

	Z	C (mole/m^3)	D (m^2/s)
Cu^{2+}	+2	10	7E-10
HSO_4^-	-1	110	1.06E-9
H^+	+1	200	9.31E-9

Table 1 : Properties of the electrolyte.

The overpotential relation describing the cathode reaction (deposition of cupper) is

$$J = J_0 \left(\frac{C}{C_n} \right)^{\gamma} \left(e^{a \frac{zF}{RT} h} - e^{-b \frac{zF}{RT} h} \right) \qquad (32)$$

with J_0= 5 Am^{-2}, $\alpha = 0.25$, $\beta = 0.25$, T = 300 K and Z = 2. C is the concentration at the electrode of the reacting ion, C_n the bulk concentration of the reacting ion equal to 10 mole/m^3 and γ is chosen to be equal to 1.

Using these data, the concentration, potential and current density distribution for different fractions of the limiting current are calculated in a turbulent fluid flow of Re = 3300. As the turbulence model for the mass transfer, $Sc_T = 1$ for all ions was used.

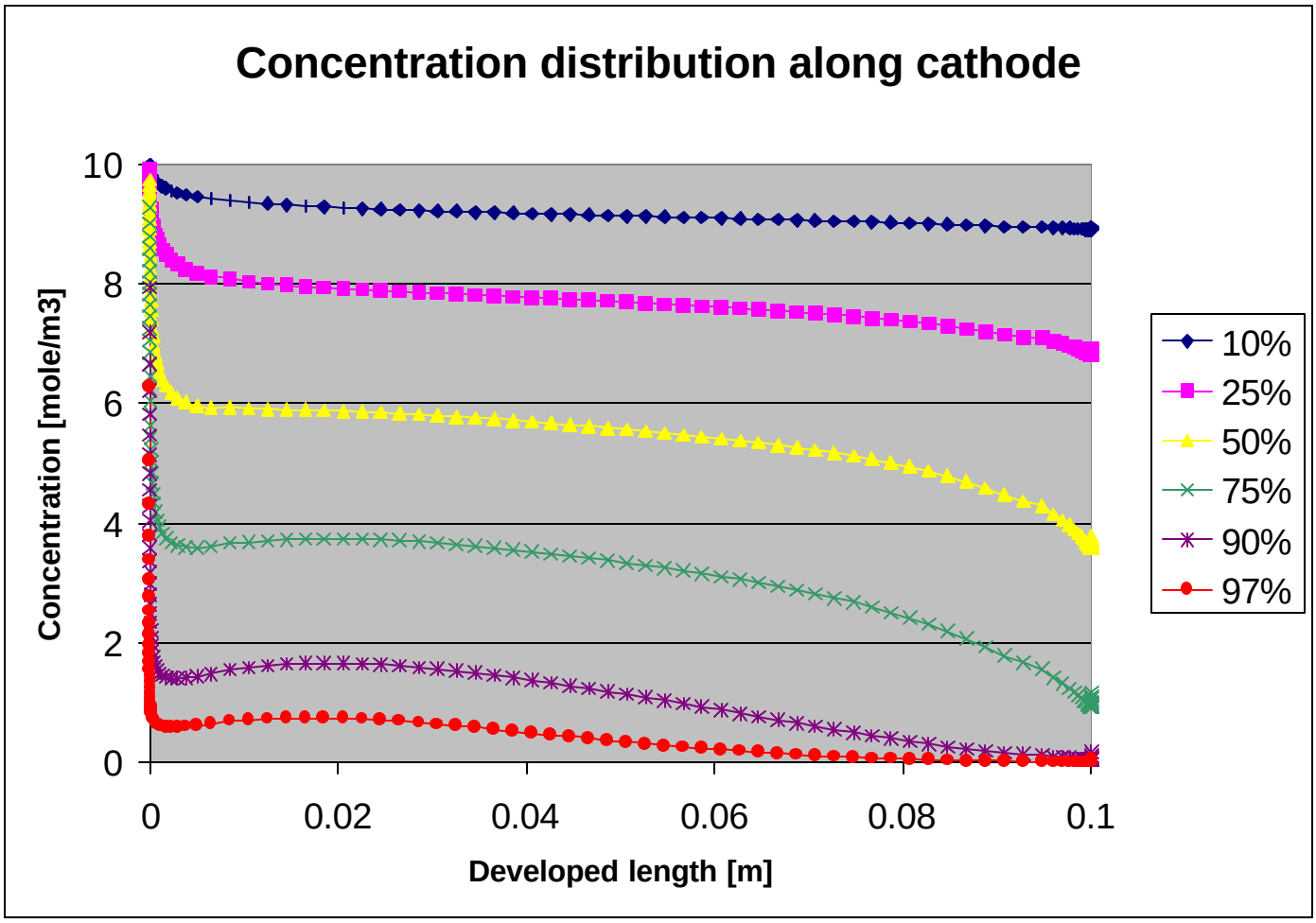

Figure 9 : Concentration distribution along the cathode for different fractions of the total limiting current.

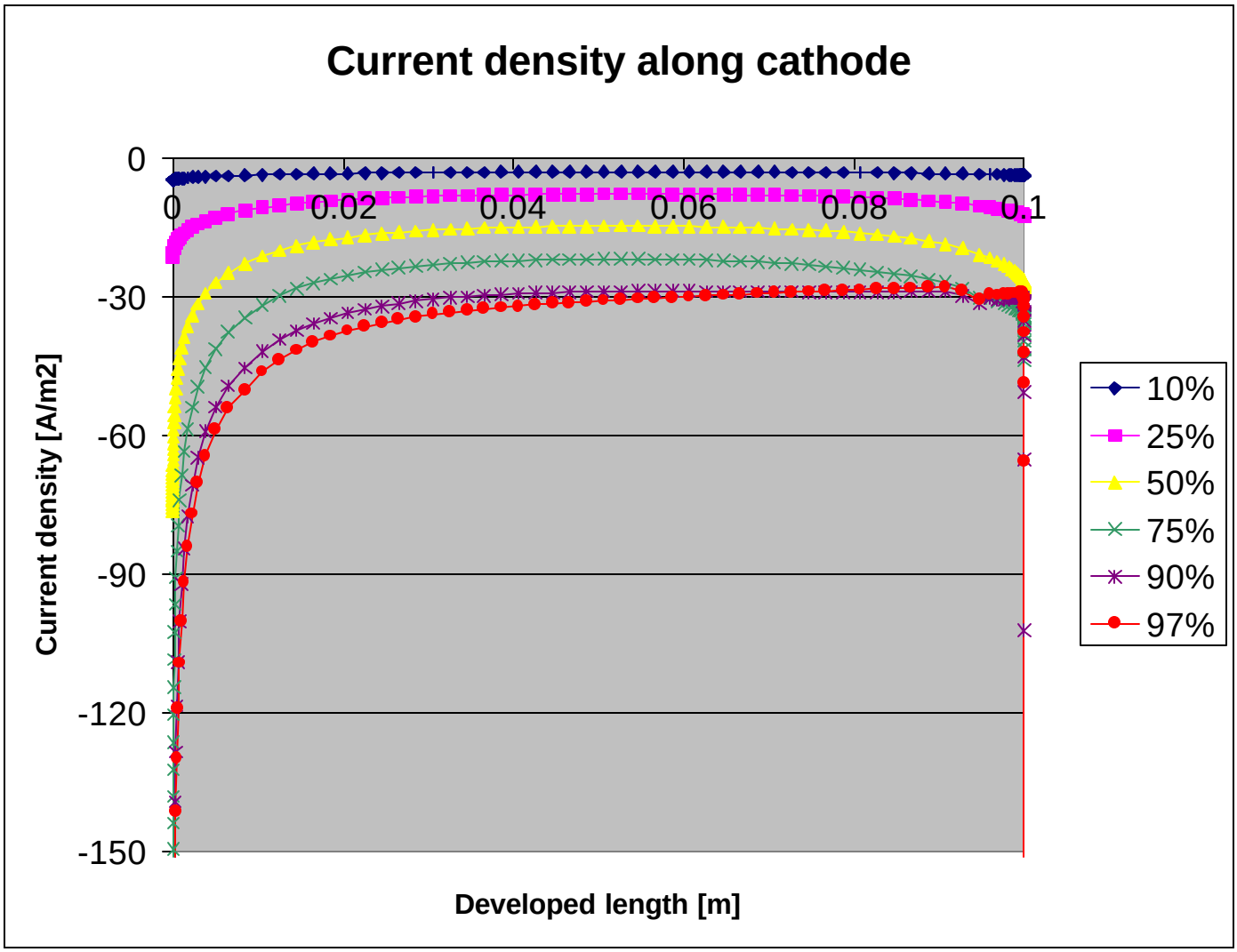

Figure 10 : Current density distribution along the cathode for different fractions of the total limiting current.

Figure 9 shows the concentration distribution along the cathode for different fractions of the limiting current. As expected, the downstream part of the cathode reaches the limiting current density regime first, because the boundary layer increases in thickness along the cathode. It is important to note that even at 75% of the total limiting current, no part of the cathode is in limiting current. At the leading edge of the cathode, the edge effect (very high current density) will sharply decrease the concentration of the reacting ion. Remark also the 'bump' in the concentration profile for the total current between 50% and 97% of the limiting current. This is due to a competition between increase in the concentration by diffusion of ions through the boundary layer and decrease in concentration due to the deposition reaction. As long as the boundary layer is quite thin, the diffusive transport will be dominant and the concentration will rise, but at a certain point along the cathode, the boundary layer becomes too thick and then the concentration starts decreasing. For the lower currents, the edge effect doesn't create a concentration gradient large enough to have an increase in concentration due to diffusion.

In Figure 10, the current density along the cathode for different fractions of the limiting current is shown. It is clear that mass transfer only start playing an important role at 50 % or higher of the limiting current.

Conclusions

Calculation of turbulent mass transfer in a parallel plate reactor were performed and validated with correlations found in literature. Different turbulence models have been studied, showing that the model of Rosen and the proposed $Sc_T = 4.5$ give the best results for this test case. Both neglecting the turbulent diffusion as extrapolating the turbulent Schmidt number from heat transfer, give unacceptable results, even for this very simple geometry. However, still a lot of research needs to be done, before simulations will be able to accurately predict turbulent mass transfer in arbitrary geometries, for a wide range of Sc and Re numbers.

References

[1] David C. Wilcox, *Turbulence Modelling for CFD*, DCW Industries, 2nd edition, 1998.
[2] A.J. Reynolds, *International Journal of Heat and Mass Transfer*, **1055-1069**, 1975.
[3] J.S. Son & T.J. Hanratty, *A I Ch E Journal*, **689-696**, 1967.
[4] J. Kim., P. Moin & R. MOSER, *J. Fluid Mech.,* **133**, 1987.
[5] N.N. Mansour, J. Kim & P. Moin (1988), *J. Fluid Mech*., **15**, 1988.
[6] C. Rosen, C. Tragardh, *The Chemical Engineering Journal,* **153-159**, 1995.
[7] S. Aravinth, *International Journal of Heat and Mass Transfer,* **1399-1408**, 2000.
[8] L. Bortels, J. Deconinck, B. Van Den Bossche; *Journ. of Electroanal. Chem.*, **15-26**; 1996.
[9] A.F. Averill, H.S. Mahmood, *Trans. IMF,* **11,** 1996
[10] D. Landolt, R.H. Muller, C.W. Tobias, *J. Electrochem. Soc.*, **1384**, 1969